View metadata, citation and similar papers at core.ac.uk

brought to you by CORE

provided by University of Queensland eSpace

Accepted Manuscript

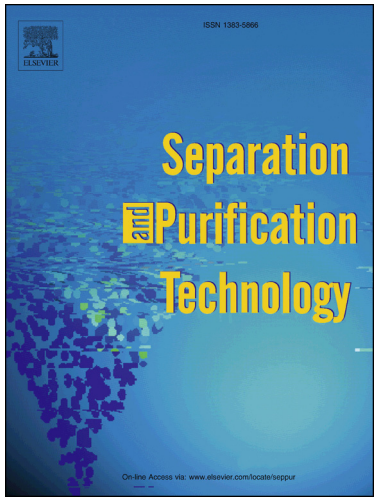

Fine ultra-micropore control using the intrinsic viscosity of precursors for high performance carbon molecular sieve membranes

Guotong Qin, Xiaofen Cao, Hua Wen, WeiWei, João C. Diniz da Costa

PII: S1383-5866(16)32252-3
DOI: http://dx.doi.org/10.1016/j.seppur.2016.12.047
Reference: SEPPUR 13458

To appear in: *Separation and Purification Technology*

Received Date: 3 November 2016
Revised Date: 30 December 2016
Accepted Date: 30 December 2016

Please cite this article as: G. Qin, X. Cao, H. Wen, WeiWei, J.C. Diniz da Costa, Fine ultra-micropore control using the intrinsic viscosity of precursors for high performance carbon molecular sieve membranes, *Separation and Purification Technology* (2016), doi: http://dx.doi.org/10.1016/j.seppur.2016.12.047

This is a PDF file of an unedited manuscript that has been accepted for publication. As a service to our customers we are providing this early version of the manuscript. The manuscript will undergo copyediting, typesetting, and review of the resulting proof before it is published in its final form. Please note that during the production process errors may be discovered which could affect the content, and all legal disclaimers that apply to the journal pertain.

ACCEPTED MANUSCRIPT

Fine ultra-micropore control using the intrinsic viscosity of precursors for high performance carbon molecular sieve membranes

Guotong Qin[1, *], Xiaofen Cao[1], Hua Wen[1], Wei Wei[2], João C. Diniz da Costa[3]

[1] School of Space and Environment, Beihang University, 37 Xueyuan Road, Beijing, China.

[2] College of Arts and Science, Beijing Union University, 197 Beituchengxi Road, Beijing, China.

[3] The University of Queensland, FIM[2]Lab – Functional Interfacial Materials and Membranes Laboratory, School of Chemical Engineering, Brisbane, Qld 4072, Australia.

Abstract

Here we report the permeability and separation performance of self-standing carbon molecular sieve (CMS) membranes formed by pyrolysis of polyimide (PI) precursors derived from poly(amic acid) (PAA) with varying intrinsic viscosity. CMS resulted in ultra-microporous membranes showing a classical molecular sieving structure as gas permeation was high for smaller molecular gas (H_2), which then decreased sequentially as the molecular sizes increased in the order of CO_2, O_2 and N_2. An important relationship was found when the intrinsic viscosity of the PAA precursor decreased from 1.66 to 0.65 dl g^{-1}, the ideal gas selectivity jumped to higher values such as from 101.8 to 163.1 for H_2/N_2, from 21.5 to 34.6 for CO_2/N_2 and from 6.7 to 10.7 for O_2/N_2 while the permeability decreased such as from 1816 to 1487 Barrer for H_2, from 383.4 to 314.8 Barrer for CO_2, from 119.0 to 97.7 Barrer for O_2, from 17.8 to 9.1 Barrer for N_2. The low intrinsic viscosity conferred a superior pore size control of the CMS structure, with an average ultramicropore size around 3Å. The O_2/N_2 and H_2/N_2 ideal selectivity versus permeability results were all above the Robeson's upper bound line, thus demonstrating the effect of low intrinsic viscosity precursors in

* Corresponding author. E-mail: qingt@buaa.edu.cn (Guotong Qin); Tel +86-10 82338556

ACCEPTED MANUSCRIPT

the synthesis of high performance CMS membranes.

Keywords Carbon molecular sieve membrane; Gas separation; Intrinsic viscosity of precursor; Ultramicropores.

1. Introduction

Carbon membranes have attracted a great deal of attention from the research community and industry due to an easy membrane fabrication process, good pore size control and excellent chemical stability. Carbon membranes are generally synthesised from pyrolysis of polymer precursors. These are often known as carbon molecular sieve (CMS) membranes. Therefore, the characteristics of polymer precursor and carbonisation process affect the structure and performance of CMS membranes. There is an array of polymers that have been employed for the preparation of CMS membranes including phenolic resin [1-7], polyimide (PI) [8-17], polyfurfuryl alcohol [18, 19], poly (2,6-dimethyl-1,4-phenylene oxide) (PPO) [20] and poly (phthalazinone ether sulfone ketone) (PPESK) [21]. In addition, carbon templates such as triblock copolymers [22] and surfactant hexyltriethylammonium bromide (C6) [23] have been embedded and carbonised in silica films as molecular sieve structures for desalination and gas separation. Alumina nano wires and silver nanoparticles have been used to improve the performance of CMS membranes [24-26].

Many of the studies reported in the literature have investigated carbon membranes based on the effect of different chemical structures such as sulfonated phenolic resin [27] and poly(furfuryl alcohol) (PFA) [28], or polyimides synthesised with a varying number of carboxylic acid groups [29]. Other studies focused on the effect of cross linking agents on the precursor structure including sulfonated poly (phthalazinone ether sulfone ketone) (SPPESK) [30] and Matrimid® 5218 [31]. During pyrolysis, the polymer precursor undergoes a complex process including thermal decomposition, thermal deformation, condensation and aromatisation. Even for a thermosetting

ACCEPTED MANUSCRIPT

polymer, partial fusion occurs during pyrolysis. The lower molecular weight polymer possesses greater chain mobility and fractional free volume than the higher molecular weight polymer. Viscosity is one of the most widely used methods for the characterization of the molecular weight of polymers, as this method provides the easiest and most rapid means of obtaining molecular weight-related data that require minimal instrumentation [32]. These characteristics are expected to affect structural rearrangement, pore formation of the CMS membranes during carbonisation, and determine the separation performance.

In this work, we investigate the synthesis of CMS membranes by carbonisation of polyimide (PI) precursor from poly (amic acid) (PAA). An important aspect of this study is understanding the effect played by varying the intrinsic viscosity (and likewise the molecular weight) of the resultant polymer precursor. PAA was synthesised from pyromelliticdianhydride (PMDA) and 4,4-oxydianiline (ODA) with phthalic anhydride (PA) end-capping to control the intrinsic viscosity. The as prepared PI and as-carbonised CMS materials were fully characterised to determine their structural properties. CMS membranes prepared with varying intrinsic viscosity precursors were tested for gas (H_2, CO_2, O_2 and N_2) permeability and their ideal gas selectivity was calculated.

2. Experimental

2.1 Materials and synthesis

PMDA (pyromelliticdianhydride) and ODA (4, 4-oxydianiline) were purchased from Sinopharm Chemical Reagent Co. Ltd. PMDA was dried at 160 °C before use and ODA was purified by re-crystallisation using ethanol as solvent. PA (phthalic anhydride) (AR) was procured from Xilong Chemical Co., Ltd. *N,N*-dimethylacetamide (DMAC) (AR) was obtained from Beijing Chemical Factory.

The synthesis of PAA and PI were schematically illustrated in Fig. 1.

ACCEPTED MANUSCRIPT

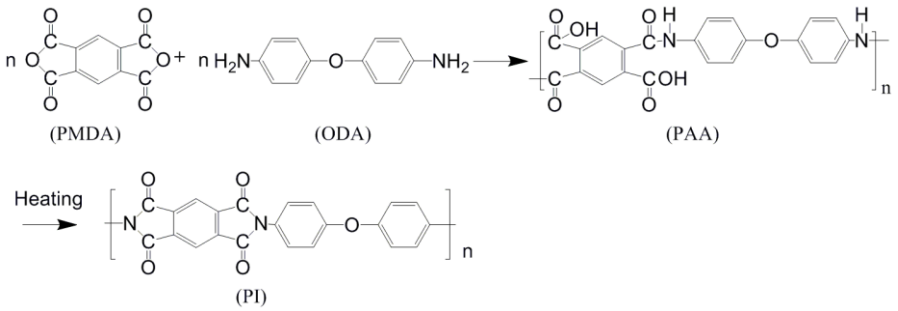

Fig. 1 Schematic illustration of synthesis of PAA and PI.

ODA was dissolved in DMAC in a three-necked flask with a stirrer and was isolated from air by a drying tube. When the solution was completely dissolved, PA (end-capping reagent) was added to the solution to control the intrinsic viscosity. Then the PMDA was added into the solution by three times, each time a third. The solution was stirred for 8 hours at room temperature. The resultant poly (amic acid) PAA solution was kept at 0–5 °C.

2.2 Preparation of PI and CMS membranes

The solution was coated on a clean glass plate using an automatic coating machine (Sheen 1132N, UK) with an applicator of width 100 mm and dried at 80 °C for 24 hours, then at 150 °C for 1 hour to prepare the PAA membranes. The PI membranes were obtained after imidising the PAA membranes with a three-step protocol: 100 °C for 30 min, 200 °C for 30 min and 300 °C for 1 h, always at a heating rate of 2 °Cmin^{-1}. The CMS membranes were prepared by carbonising the PI membranes in an inert high purity argon atmosphere. The PI membranes were heated at a rate of 2 °C min^{-1} and held at 100 °C, 200 °C, 300 °C, and 400 °C for 30 min respectively, before heating to 700 °C at a rate of 1 °C min^{-1} for 60 min. The CMS membranes generally had a thickness of 35–37 microns. The thickness was measured by a micrometer thickness gauge (CH-1-S, Shanghai Liuling Instrument, Shanghai, China).

2.3 Characterisation

A STA449C (Simultaneous Thermogravimetry – Differential Scanning Calorimetry, Netzsch,

ACCEPTED MANUSCRIPT

Germany) was used to test the thermal stability, mass loss with temperature, and the glass transition temperature (T_g) of the membranes, under an argon gas flow of 30 ml min^{-1} and a heating rate of 10 °C min^{-1}. Nitrogen and carbon dioxide sorption at 77 K and 273.15 K were conducted on an ASAP 2020 (Micromeritics, USA). The ASAP 2020 software from Micromeritics Instrument Corporation, based on non-local density functional theory, was used to analyse N_2 and CO_2 sorption isotherms to aid in characterisation of pore size of CMS membranes. The analysis involved estimating the adsorption for pores of a particular characteristic size. The intrinsic viscosity was measured using an Ubbelohde viscometer at 25°C.

2.4 CMS membrane testing

Single gas permeability of the CMS membranes was tested by a dead-end set up using a time-lag method[19]. A setting for testing is shown in Fig.2. A pressure gradient was generated across the membrane with a gas cylinder upstream and a vacuum downstream. The volume of the module was measured for both the feed side and the permeation side. Two pressure transducers were used to monitor the change of the pressure of the feed side and permeation side. The membrane was supported by a porous stainless steel disc to protect it from cracking during testing. The permeability was calculated according to the time rate of change in permeate side pressure

$$\frac{V_{ps}}{ART}\ln\frac{|P_{fs}-P_{ps0}|}{|P_{fs}-P_{ps}|}=\frac{\pi}{\delta}t \qquad (1)$$

where V_{ps} is the permeate side volume; P_{fs} and P_{ps} are the pressures on the feed side and permeation side of the membrane, respectively; P_{ps0} is the initial permeation side pressure; π is the gas permeability (mol $m^{-1}sec^{-1}Pa^{-1}$); δ is the membrane thickness; and t is the time. A straight line can be obtained from plot of the equation 1, left side versus time. The slope π/δ is the permeance (mol $m^{-2}sec^{-1}Pa^{-1}$).

ACCEPTED MANUSCRIPT

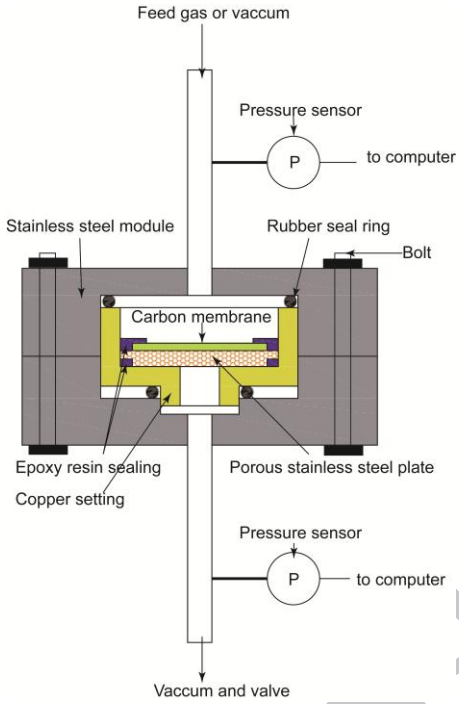

Figure 2 Schamatic diagram of the setting for test of gas permeance of CMS membranes.

3. Results and discussion

The intrinsic viscosity of the synthesised PAA is shown in Table 1. The intrinsic viscosity was controlled by addition of end-capping reagent PA. The PAA precursors, PI membranes and CMS membranes were labelled according to their intrinsic viscosity. Fig. 3 shows the glass transition temperature (T_g) of PI membranes versus the intrinsic viscosity of the PAA precursors. The T_g of PI marginally decreased from 318 to 315 °C as the intrinsic viscosity was reduced from 1.66 to 0.95 dl g^{-1}, respectively. This T_g marginal decrease was not significant and within experimental error of 3%. The onset of T_g decrease was observed at PI-95 (0.95 dl g^{-1}) and then became significant with the T_g decreasing to 276 °C for PI-17 (0.17 dl g^{-1}). It should be noted that the PAA-17 was so brittle that it was not possible to prepare membranes. The low T_g value implied that the PI needed less energy to rearrange the structure of the polymer chains during heat treatment.

ACCEPTED MANUSCRIPT

Table 1 PAA membrane ID and the viscosity of the PAA precursor

PAA samples	Intrinsic viscosity	PMDA (mmol)	ODA (mmol)	PA(mmol)
PAA-166	1.66	120.0	120.0	0
PAA-145	1.45	120.0	120.0	1.7
PAA-95	0.95	120.0	120.0	5.1
PAA-65	0.65	120.0	120.0	8.7
PAA-17	0.17	120.0	120.0	63.5

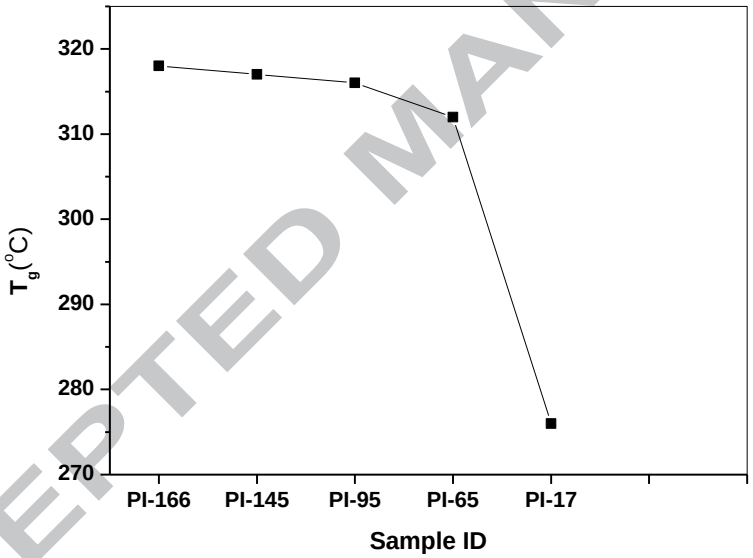

Figure 3. Glass-transition temperature of PI versus the intrinsic viscosity of the PAA precursor.

The decomposition of the PI samples under pyrolysis is displayed in Fig. 4. The decomposition temperatures for PI-166 to PI-65 occurred at 550 °C except the PI-17 which began to decompose at a much lower temperature of 350 °C. Overall, the weight loss slightly increased as the intrinsic viscosity decreased for all samples. The lower intrinsic viscosity (i.e. lower molecular weight) polymer is associated with lower carbon yield, leading to weaker inter-chain forces and stronger

ACCEPTED MANUSCRIPT

chain mobility during pyrolysis. It is observed that the PI-17 showed a two-stage weight loss. This low thermal stability could be correlated to the intrinsic viscosity of PI-17 which was much lower than the other PI samples, leading to decomposition at lower temperatures.

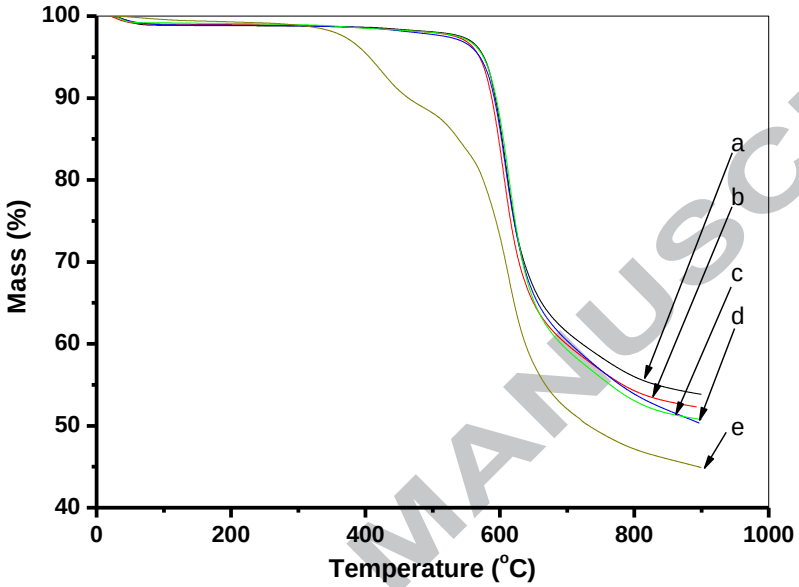

Figure 4. Mass loss of different samples during pyrolysis (a) PI-166, (b) PI-145, (c) PI-95, (d) PI-65, (e) PI-17.

Figs.5a and 5b show the N_2 and CO_2 sorption isotherms of CMS powders derived from PI with varying intrinsic viscosity. The N_2 sorption isotherms are characterised by sorption uptakes at very low relative pressures of $P/P_o < 0.05$ where sorption saturation was reached. These are type I isotherms, characteristic of microporous materials. This is reflected by the pore size distribution plot in Fig. 5c, where microporosity is observed, while meso and macroporosity are absent. The majority of the pore sizes are in the ultra-micropore region below 0.45 nm. The CMS-17 shows the highest relative incremental volume below 0.45 nm, thus indicating that precursors with low intrinsic viscosity had a propensity to form a higher volume of ultra-micropores. Further, the formation of ultra-micropores is evidenced by the pore volumes (by Dubinin-Radushkevich (DR) model) of the CO_2 isotherms being always higher than those from N_2 isotherms as listed in Table 2.

ACCEPTED MANUSCRIPT

This is attributed that at 77 K N_2 generally does not access ultra-micropores, which can be measured by CO_2 at 273.15 K. However, as shown in Table 3, there is no relationship between the intrinsic viscosity of precursor and the surface area of the CMS membranes.

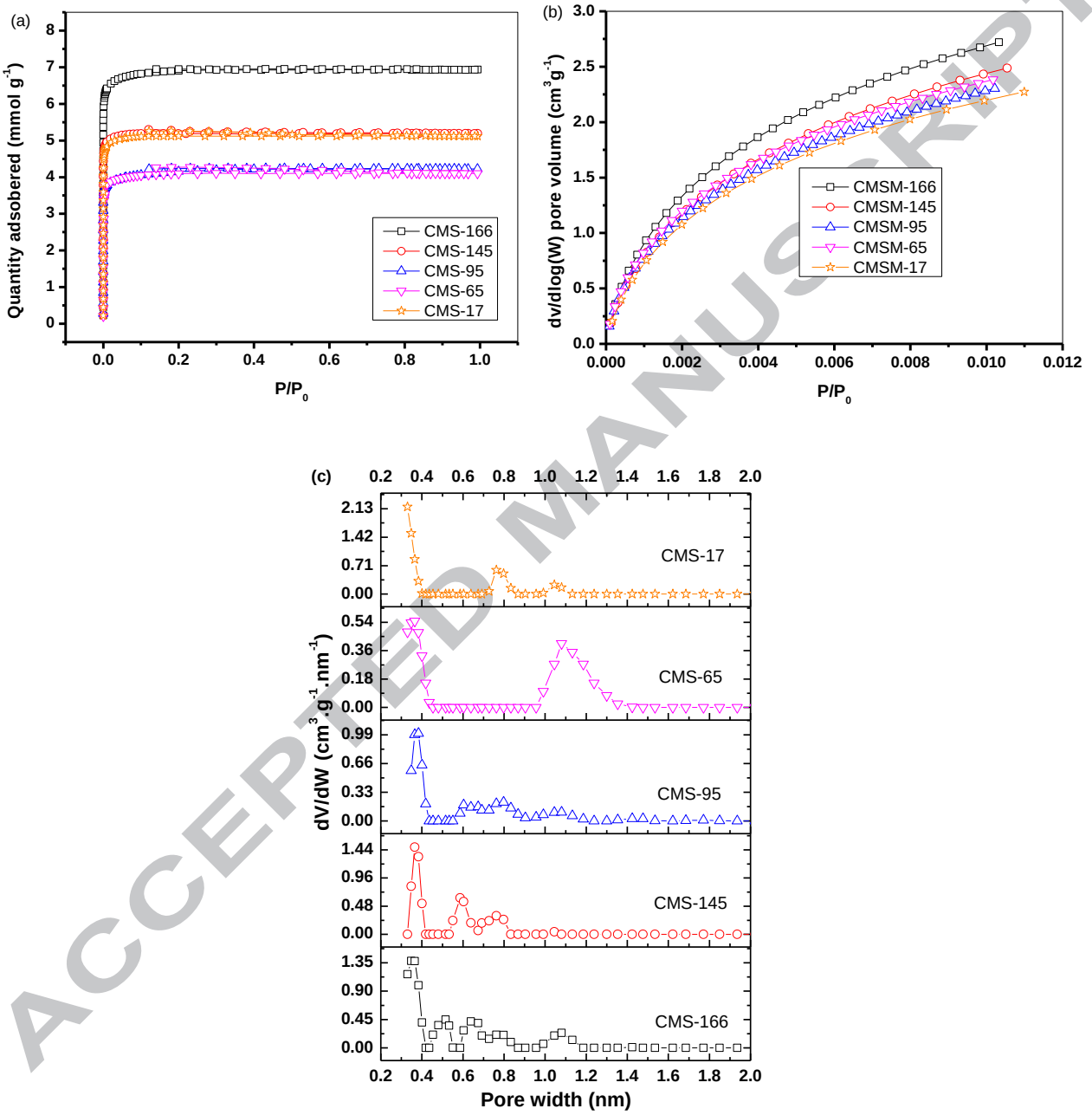

Figure 5. Isotherms of (a) nitrogen adsorption and (b) carbon dioxide adsorption, and (c) pore size distributions of CMS membranes prepared with precursors with different intrinsic viscosity.

ACCEPTED MANUSCRIPT

Table 2.Micropore volume from N_2 and CO_2 adsorption by DR Model (cm^3g^{-1})

Adsorbate	PAA-166	PAA-145	PAA-95	PAA-65	PAA-17
N_2	0.238	0.183	0.141	0.156	0.181
CO_2	0.276	0.255	0.221	0.230	0.230

Table 3 BET surface area of the CMS membranes ($m^2.g^{-1}$)

PAA-166	PAA-145	PAA-95	PAA-65	PAA-17
518	375	313	308	382

CMS membranes are crack free as shown in Figure S1. All the CMS membranes were tested for single gas permeation at room temperature using a dead-end permeation set up. Fig. 6a shows a classical behavior of molecular sieving membranes, where there is an order of higher permeability from the molecules with the smaller kinetic diameter H_2 (d_k = 2.89Å), which reduces as the molecular sizes increase to CO_2 (d_k = 3.3 Å), O_2 (d_k = 3.46 Å) and N_2 (d_k = 3.64Å). CMS membranes delivered very high H_2 permeabilities of 1500–2000 Barrer, which reduced by two orders of magnitude for the largest molecular size gas tested (N_2). The effect of intrinsic viscosity (and likewise molecular weight) can be clearly observed by plotting this parameter against the ideal selectivity in Fig. 6b, which consistently shows that an increase in the ideal selectivity was accompanied by the decrease of the intrinsic viscosity. When the intrinsic viscosity of the PAA precursor decreased from 1.66 to 0.65 dl g^{-1}, the ideal selectivity jumped to higher values such as from 101.8 to 163.1 for H_2/N_2, from 21.5 to 34.6 for CO_2/N_2 and from 6.7 to 10.7 for O_2/N_2.

ACCEPTED MANUSCRIPT

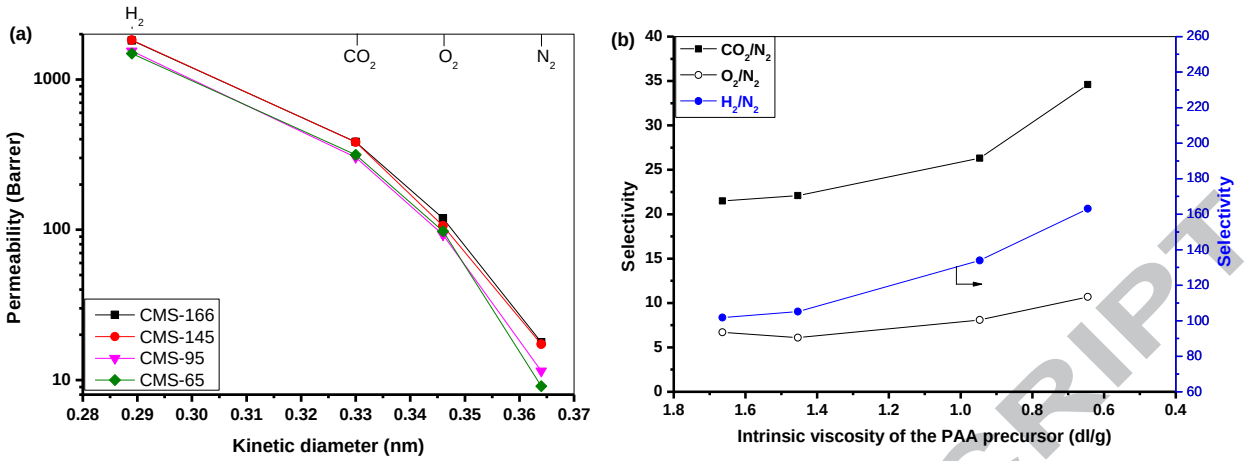

Figure 6. (a) Single gas permeability and (b) ideal selectivity for CMS membranes prepared with PI precursors with varying intrinsic viscosity. (1 Barrer=1×10^{-10}cm^3(STP) cm cm^{-2}s^{-1}cmHg^{-1}, the permeability from 3-5 samples with error less than 10%).

These results strongly indicate that the low intrinsic viscosity precursor was able to tailor pore sizes smaller than the kinetic diameter of N_2. There is a good correlation between the increase of H_2 permeability over the other tested gases and the pore size distribution in Fig. 5c, which shows a relative higher ultra-microporous volume for the low intrinsic viscosity precursor. The CMS membranes prepared in this work delivered high performance in terms of both permeability and ideal selectivity. This can be seen by the Robeson's plots in Fig. 7. The H_2/N_2 separation is well above Robeson's upper bound, thus demonstrating the potential of this membrane for applications involving the separation of H_2 from gas stream in processes involving air blown coal or biomass gasification. The separation of O_2/N_2 is less impressive, though still above the Robeson's upper bound, demonstrating that the separation of oxygen from air is always a low yield process using porous[33] or polymeric[34] membranes.

ACCEPTED MANUSCRIPT

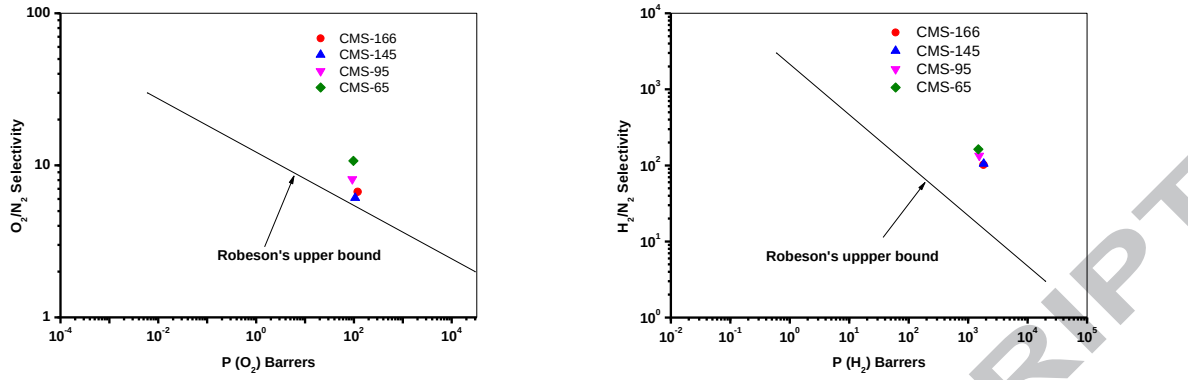

Figure 7. Selectivity of CMS membranes versus Robeson upper bound[35]shows the trade-off from current polymers.

4. Conclusion

High selective CMS membranes were prepared by the carbonization of polyimide from PMDA and ODA. The intrinsic viscosity of the PAA precursor was controlled by end-capping reagent PA. A series of PAA were synthesized with inherent viscosity 0.17–1.66 dl g^{-1} to study the effects of the precursor intrinsic viscosity on the gas separation of CMS membranes. This work shows a good correlation between the intrinsic viscosity of the PAA precursors and the performance of the CMS membranes. Low intrinsic viscosity PAA increased the ultramicropore fraction and enhanced the gas selectivity of the CMS membranes. The CMS membrane prepared from PAA with intrinsic viscosity 0.65 dl g^{-1}delivered separation factors of 10.7 for O_2/N_2 and 163.1 for H_2/N_2, and permeabilities of 97.7 Barrer for O_2 and 1487 Barrer for H_2. These results are above the Robeson's upper bound.

Acknowledgments

The authors are thankful for the financial support given by the National Science Foundation of China (Project 51272104, 51172027). J. C. Diniz da Costa acknowledges support via the Australian Research Council Future Fellowship (FT130100405).

References

ACCEPTED MANUSCRIPT

[1] P.S. Lee, D. Kim, S.E. Nam, R.R. Bhave, Carbon molecular sieve membranes on porous composite tubular supports for high performance gas separations, Micropor Mesopor Mat, 224 (2016) 332-338.
[2] G.T. Qin, C. Wang, W. Wei, Preparation of a mesoporous carbon membrane from resorcinol and formaldehyde, Carbon, 48 (2010) 4206-4208.
[3] W. Wei, H.Q. Hu, L.B. You, G.H. Chen, Preparation of carbon molecular sieve membrane from phenol-formaldehyde Novolac resin, Carbon, 40 (2002) 465-467.
[4] W. Wei, G.T. Qin, H.Q. Hu, L.B. You, G.H. Chen, Preparation of supported carbon molecular sieve membrane from novolac phenol-formaldehyde resin, J Membrane Sci, 303 (2007) 80-85.
[5] T.A. Centeno, A.B. Fuertes, Carbon molecular sieve membranes derived from a phenolic resin supported on porous ceramic tubes, Sep Purif Technol, 25 (2001) 379-384.
[6] M.A.L. Tanco, D.A.P. Tanaka, S.C. Rodrigues, M. Texeira, A. Mendes, Composite-alumina-carbon molecular sieve membranes prepared from novolac resin and boehmite. Part I: Preparation, characterization and gas permeation studies, Int J Hydrogen Energ, 40 (2015) 5653-5663.
[7] M.A.L. Tanco, D.A.P. Tanaka, A. Mendes, Composite-alumina-carbon molecular sieve membranes prepared from novolac resin and boehmite. Part II: Effect of the carbonization temperature on the gas permeation properties, Int J Hydrogen Energ, 40 (2015) 3485-3496.
[8] A.C. Lua, J.C. Su, Effects of carbonisation on pore evolution and gas permeation properties of carbon membranes from Kapton((R)) polyimide, Carbon, 44 (2006) 2964-2972.
[9] Y. Song, D.K. Wang, G. Birkett, W. Martens, M.C. Duke, S. Smart, J.C. Diniz da Costa, Mixed Matrix Carbon Molecular Sieve and Alumina (CMS-Al2O3) Membranes Scientific Reports, (2016).
[10] K. Wang, H. Suda, K. Haraya, The characterization of CO2 permeation in a CMSM derived from polyimide, Sep Purif Technol, 31 (2003) 61-69.
[11] Y.J. Fu, K.S. Liao, C.C. Hu, K.R. Lee, J.Y. Lai, Development and characterization of micropores in carbon molecular sieve membrane for gas separation, Micropor Mesopor Mat, 143 (2011) 78-86.
[12] S.L. Fu, E.S. Sanders, S.S. Kulkarni, G.B. Wenz, W.J. Koros, Temperature dependence of gas transport and sorption in carbon molecular sieve membranes derived from four 6FDA based polyimides: Entropic selectivity evaluation, Carbon, 95 (2015) 995-1006.
[13] S.L. Fu, E.S. Sanders, S.S. Kulkarni, W.J. Koros, Carbon molecular sieve membrane structure-property relationships for four novel 6FDA based polyimide precursors, J Membrane Sci, 487 (2015) 60-73.
[14] D.Q. Vu, W.J. Koros, S.J. Miller, High pressure CO2/CH4 separation using carbon molecular sieve hollow fiber membranes, Ind Eng Chem Res, 41 (2002) 367-380.
[15] M. Kiyono, P.J. Williams, W.J. Koros, Effect of polymer precursors on carbon molecular sieve structure and separation performance properties, Carbon, 48 (2010) 4432-4441.
[16] L.R. Xu, M. Rungta, W.J. Koros, Matrimid (R) derived carbon molecular sieve hollow fiber membranes for ethylene/ethane separation, J Membrane Sci, 380 (2011) 138-147.
[17] W.L. Qiu, L.R. Xu, C.C. Chen, D.R. Paul, W.J. Koros, Gas separation performance of 6FDA-based polyimides with different chemical structures, Polymer, 54 (2013) 6226-6235.
[18] C.J. Anderson, S.J. Pas, G. Arora, S.E. Kentish, A.J. Hill, S.I. Sandler, G.W. Stevens, Effect of pyrolysis temperature and operating temperature on the performance of nanoporous carbon membranes, J Membrane Sci, 322 (2008) 19-27.
[19] M.B. Shiflett, H.C. Foley, Ultrasonic deposition of high-selectivity nanoporous carbon membranes, Science, 285 (1999) 1902-1905.
[20] H.J. Lee, M. Yoshimune, H. Suda, K. Haraya, Gas permeation properties of poly (2,6-dimethyl-1,4-phenylene oxide) (PPO) derived carbon membranes prepared on a tubular ceramic support, J Membrane Sci, 279 (2006) 372-379.
[21] B. Zhang, L. Li, C.L. Wang, J. Pang, S.H. Zhang, X.G. Jian, T.H. Wang, Effect of membrane-casting parameters on the microstructure and gas permeation of carbon membranes, Rsc Adv, 5 (2015) 60345-60353.
[22] M. Elma, D.K. Wang, C. Yacou, J.C.D. da Costa, Inter layer-free P123 carbonised template silica membranes for

ACCEPTED MANUSCRIPT

desalination with reduced salt concentration polarisation tages, J Membrane Sci, 475 (2015) 376-383.
[23] M.C. Duke, J.C.D. da Costa, G.Q. Lu, M. Petch, P. Gray, Carbonised template molecular sieve silica membranes in fuel processing systems: permeation, hydrostability and regeneration, J Membrane Sci, 241 (2004) 325-333.
[24] M. Teixeira, S.C. Rodrigues, M. Campo, D.A.P. Tanaka, M.A.L. Tanco, L.M. Madeira, J.M. Sousa, A. Mendes, Boehmite-phenolic resin carbon molecular sieve membranes-Permeation and adsorption studies, Chem Eng Res Des, 92 (2014) 2668-2680.
[25] M. Teixeira, M. Campo, D.A. Tanaka, M.A. Tanco, C. Magen, A. Mendes, Carbon–Al 2 O 3 –Ag composite molecular sieve membranes for gas separation, Chem Eng Res Des, 90 (2012) 2338-2345.
[26] M. Teixeira, M.C. Campo, D.A.P. Tanaka, M.A.L. Tanco, C. Magen, A. Mendes, Composite phenolic resin-based carbon molecular sieve membranes for gas separation, Carbon, 49 (2011) 4348-4358.
[27] W.L. Zhou, M. Yoshino, H. Kita, K. Okamoto, Carbon molecular sieve membranes derived from phenolic resin with a pendant sulfonic acid group, Ind Eng Chem Res, 40 (2001) 4801-4807.
[28] C.W. Song, T.H. Wang, H.W. Jiang, X.Y. Wang, Y.M. Cao, J.S. Qiu, Gas separation performance of C/CMS membranes derived from poly (furfuryl alcohol) (PFA) with different chemical structure, J Membrane Sci, 361 (2010) 22-27.
[29] Y.K. Kim, J.M. Lee, H.B. Park, Y.M. Lee, The gas separation properties of carbon molecular sieve membranes derived from polyimides having carboxylic acid groups, J Membrane Sci, 235 (2004) 139-146.
[30] B. Zhang, Y.H. Wu, T.H. Wang, J.S. Qiu, S.H. Zhang, Microporous Carbon Membranes from Sulfonated Poly(phthalazinone ether sulfone ketone): Preparation, Characterization, and Gas Permeation, J Appl Polym Sci, 122 (2011) 1190-1197.
[31] S.T. Pei, T.S. Chung, S. Kawi, M.D. Guiver, Novel approaches to fabricate carbon molecular sieve membranes based on chemical modified and solvent treated polyimides, Micropor Mesopor Mat, 73 (2004) 151-160.
[32] Seymour, B. Raymond, Carraher's polymer chemistry, Taylor & Francis, 2014.
[33] R. Singh, W.J. Koros, Carbon molecular sieve membrane performance tuning by dual temperature secondary oxygen doping (DTSOD), J Membrane Sci, 427 (2013) 472-478.
[34] R.W. Baker, B.T. Low, Gas Separation Membrane Materials: A Perspective, Macromolecules, 47 (2014) 6999-7013.
[35] L.M. Robeson, The upper bound revisited, J Membrane Sci, 320 (2008) 390-400.

ACCEPTED MANUSCRIPT

ACCEPTED MANUSCRIPT

Graphical abstract

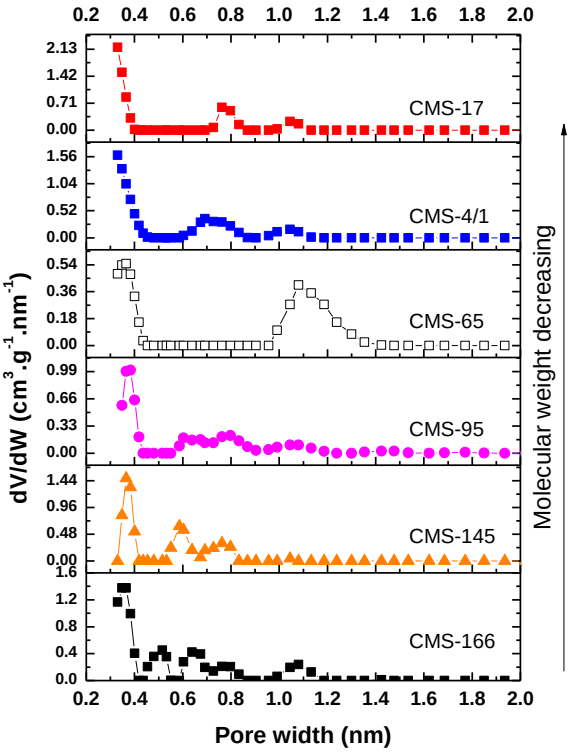

ACCEPTED MANUSCRIPT

ACCEPTED MANUSCRIPT

Highlights

- High performance carbon molecular sieve membrane for gas separation is prepared.
- Ultra-micropore structure is tailored by intrinsic viscosity of precursor.
- Precursor with low intrinsic viscosity leads to high selective CMS membranes.

ACCEPTED MANUSCRIPT